ELSEVIER

Physica B 297 (2001) 169–174

PHYSICA B

www.elsevier.com/locate/physb

Towards 3D polarization analysis in neutron reflectometry

B. Toperverg[a,b], O. Nikonov[c,d,*], V. Lauter-Pasyuk[d,e], H.J. Lauter[c]

[a]*Petersburg Nuclear Physics Institute, Gatchina, 188350 St. Petersburg, Russia*
[b]*Institut für Festkörperforschung, Forshungszentrum Jülich, D-52425 Jülich, Germany*
[c]*Institute Laue Langevin, Grenoble, France*
[d]*Joint Institute for Nuclear Research, Dubna, Moscow Region, Russia*
[e]*TU München, Physik Department, D-85747 Garching, Germany*

Abstract

General equations for spin-flip and non-spin-flip specular reflection and off-specular scattering are analyzed for the case of multidomain states of magnetic multilayers. The results are illustrated by numerical calculations performed for Fe/Cr multilayers using an original software developed on the basis of the supermatrix formalism. This routine allows to calculate the reflectivities and scattering cross sections from the layered structures of any complexity for any directions of the incident polarization vector and directions of the polarization analysis.

Keywords: 3D polarization analysis; Multilayers; Magnetic domains

1. Introduction

During the last decade polarized neutron reflectometry (PNR) has received wide recognition [1–4] as a powerful tool, which delivers the most complete information on the magnetization arrangement in thin films and multilayers. In combination with the polarized neutron off-specular scattering, it gives experimental evidences on magnetic domain arrangement and interfacial magnetic roughness [5–8]. In the mean time, the reflected and scattered intensities are measured in a single direction of the initial polarization and polarization analysis, and at most four quantities: two spin-flip and two non-spin-flip components of the reflectivity (scattering cross section) are available for theoretical evaluation. However, it is well established for bulk magnetic systems that quite often measurements at one direction of the polarization do not render a sufficient amount of information needed for the unique solution of the model. More complete information is obtained from measurements at three, usually orthogonal, directions of the polarization, providing 36 instead of four experimental quantities. This technique, called polarization vector or 3 Dimensional (3D) analysis was first developed for the direct beam and small angle scattering experiments [9,10]. Nowadays it is used in a number of diffraction and inelastic scattering measurements [11].

In the case of reflection kinematics the situation is more complicated from both experimental and theoretical points of view. One of the main

* Corresponding author.
E-mail address: nikonov@ill.fr (O. Nikonov).

0921-4526/01/$ - see front matter
PII: S0921-4526(00)00866-8

experimental problems is quite general and related to the effects of the demagnetizing field outside the sample. If this field is sufficiently homogeneous and does not lead to a noticeable spatial splitting of the neutron beam [12,13] (Stern–Gerlach effect), then the Larmor precession can either be avoided by a proper short circuit for the magnetic flux outside the neutron path, or taken into account [14]. In the simplest case one may analyze only the projections of the outgoing neutron spins onto the direction of incoming polarization, subsequently directed along each of three Cartesian axes. Usually, the conditions for non-adiabatic transmission of the neutron spin into the film can be fulfilled at any direction of weak field guiding the initial polarization, and this, 3-directional (according to Mezei), or 3D, version of 3D polarization analysis delivers 12 measurable quantities — an amount often sufficient to define a theoretical model.

In [6,7], the data of polarized neutron reflectivity and off-specular scattering measured for Fe/Cr multilayers are well described within the model of small antiferromagnetic domains. In these experiments the initial polarization vector $\boldsymbol{P}_{\rm i}$ and vector of the final polarization analysis $\boldsymbol{P}_{\rm f}$ were chosen parallel to the net magnetization of the system. In the present communication, we shall present the model calculations made for forthcoming experiments on the same system, but with the vectors $\boldsymbol{P}_{\rm i}$ and $\boldsymbol{P}_{\rm f}$ directed also along two other axis orthogonal to the magnetization and either parallel or perpendicular to the axis of antiferromagnetism. We shall demonstrate, that 3D analysis can deliver an additional information, which can be used to verify the model proposed in Ref. [6,7].

2. Reflection and scattering matrices

In Ref. [15–17], general explicit equations were derived for the reflectivity, $\mathscr{R} = \mathscr{R}(\boldsymbol{P}_{\rm f},\boldsymbol{P}_{\rm i})$, and scattering cross section, $(\mathrm{d}\sigma/\mathrm{d}\Omega)$, in the invariant form independent of the coordinate system and for an arbitrary mutual orientation between the vectors $\boldsymbol{P}_{\rm f}$ and $\boldsymbol{P}_{\rm i}$. These equations are derived using the general definitions:

$$\mathscr{R} = \mathrm{Tr}\{\hat{\rho}^{\rm i}\hat{R}^{+}\hat{\rho}^{\rm f}\hat{R}\}, \tag{1}$$

$$\frac{\mathrm{d}\sigma}{\mathrm{d}\Omega} = \mathrm{Tr}\{\hat{\rho}^{\rm i}(\hat{F}^{+}_{\rm fi})\hat{\rho}^{\rm f}\hat{F}_{\rm fi}\}, \tag{2}$$

$$\hat{\rho}^{\rm i} = \tfrac{1}{2}(1 + \boldsymbol{\sigma}\boldsymbol{P}_{\rm i}), \quad \hat{\rho}^{\rm f} = \tfrac{1}{2}(1 + \boldsymbol{\sigma}\boldsymbol{P}_{\rm f}), \tag{3}$$

where the reflectance matrix $\hat{R}$ and the scattering operator $\hat{F}_{\rm fi}$ are averaged over the spin states determined by the density matrices $\hat{\rho}^{\rm i}$ and $\hat{\rho}^{\rm f}$, which describe the properties of the polarizing or, respectively, analyzing devices, $\boldsymbol{\sigma} = 2\boldsymbol{s}_{\rm N}$ is the vector of the Pauli matrices and $\boldsymbol{s}_{\rm N}$ is the neutron spin operator.

The reflectance, $\hat{R} = \hat{R}(\boldsymbol{\sigma})$, and the scattering, $\hat{F}_{\rm fi} = \hat{F}(\boldsymbol{\sigma})$, operators can formally be expanded [15], similar to Eq. (3), over a set of the Pauli matrices:

$$\hat{R} = R_0 + (\boldsymbol{R}\boldsymbol{\sigma}), \quad \hat{F}_{\rm fi} = F_0 + (\boldsymbol{F}\boldsymbol{\sigma}), \tag{4}$$

where $R = (\frac{1}{2})\mathrm{Tr}\{\hat{R}\}$, $\boldsymbol{R} = (\frac{1}{2})\mathrm{Tr}\{\hat{\boldsymbol{R}}\boldsymbol{\sigma}\}$, $F_0 = (\frac{1}{2})\mathrm{Tr}\{\hat{F}_{\rm fi}\}$, $\boldsymbol{F} = (\frac{1}{2})\mathrm{Tr}\{\hat{\boldsymbol{F}}_{\rm fi}\boldsymbol{\sigma}\}$. For scattering from a multilayer $\hat{F}_{\rm fi} = \sum_{\rm l}\hat{F}^{\rm l}(\boldsymbol{Q}_{||},\hat{p}^{\rm l}_{\rm f},\hat{p}^{\rm l}_{\rm i};\boldsymbol{\sigma})$, where l enumerates layers, $\boldsymbol{Q}_{||}$ is the lateral momentum transfer, $\hat{p}^{\rm l}_{\rm f,i}$ are the operators of the wave vector components normal to the surface.

Substitution of Eqs. (4) into Eqs. (1)–(3) gives the equations for $\mathscr{R}$ and $\mathrm{d}\sigma/\mathrm{d}\Omega$ [15–17], which we reproduce here in a particular coordinate system for the model proposed in Ref. [6] and depicted in Fig. 1. We assume that the mean magnetization in

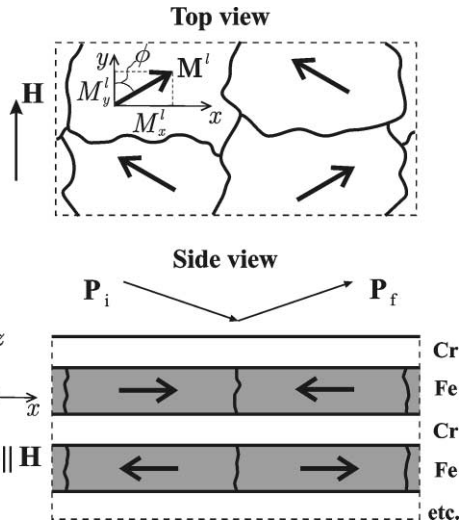

Fig. 1. Sketch of the domain magnetization (thick arrows) arrangement of the $[[\mathrm{Cr}(9\ \text{Å})/^{57}\mathrm{Fe}(68\ \text{Å})]\times 12]/\mathrm{Al_2O_3}$ multilayer.

each layer is directed along the field applied within the surface plane along the Y-axis (perpendicular to the reflection plane), and the Z-axis is orthogonal to the surface (see Fig. 1). The mean magnetization $\boldsymbol{M}$ contributes to the specular reflection, while the components of the domain magnetic moments perpendicular to $\boldsymbol{M}$, cause off-specular scattering. Due to the mean magnetic field, the neutron waves (transmitted and reflected at the interfaces) are birefringent inside each layer in accordance with the Zeeman splitting of the neutron spin states. The spin components of a neutron wave propagate, inside a layer with, the wave vectors $p^{\mathrm{l}}_{\pm} = \{p_0^2 - p^2_{\mathrm{c}\pm}\}^{1/2}$ (the eigenvalues of $\hat{p}^{\mathrm{l}}$), where $p_0 = p_0^{\mathrm{f,i}}$ is the incoming or scattered wave vector projection onto the normal to the surface, and $p_{\mathrm{c}\pm} = p^{\mathrm{l}}_{\mathrm{c}\pm}$ are the critical wave vectors of the total reflection: $p^2_{\mathrm{c}\pm} = p^2_{\mathrm{cN}} \pm p^2_{\mathrm{cM}}$ for that or the other spin component. Those components are transmitted into the layer with the amplitude $t^{\mathrm{l}}_{\pm}$, or reflected from its interface with the amplitude $r^{\mathrm{l}}_{\pm}$, which are the eigenvalues of the transmission, $\hat{t}^{\mathrm{l}} = t^{\mathrm{l}} + (\boldsymbol{t}^{\mathrm{l}}\boldsymbol{\sigma})$, and reflection, $\hat{r}^{\mathrm{l}} = r^{\mathrm{l}} + (\boldsymbol{r}^{\mathrm{l}}\boldsymbol{\sigma})$, operators represented similar to Eq. (4). All these amplitudes, including the reflectance $R_{\pm} = r^0_{\pm}$ for the whole multilayer, can easily be found via an ordinary matrix routine, and $t^{\mathrm{l}} = (t^{\mathrm{l}}_{+} + t^{\mathrm{l}}_{-})/2$, $\boldsymbol{t}^{\mathrm{l}} = (t^{\mathrm{l}}_{+} - t^{\mathrm{l}}_{-})\boldsymbol{b}/2$, $r^{\mathrm{l}} = (r^{\mathrm{l}}_{+} + r^{\mathrm{l}}_{-})/2$, $\boldsymbol{r}^{\mathrm{l}} = (r^{\mathrm{l}}_{+} - r^{\mathrm{l}}_{-})\boldsymbol{b}/2$, where $\boldsymbol{b}$ is a unit vector along the mean magnetization.

As soon as the (complex) eigenvalues $R_{\pm} = |R_{\pm}|\exp(\mathrm{i}\chi^r_{\pm})$ are found, one can substitute $R = (R_{+} + R_{-})/2$, $\boldsymbol{R} = (R_{+} - R_{-})\boldsymbol{b}/2$ in Eq. (4) and calculate the reflectivity matrix $\mathscr{R}^{\alpha\beta}_{\pm\pm} = \mathscr{R}(\pm P^{\alpha}_{\mathrm{f}}, \pm P^{\beta}_{\mathrm{i}})$ and $\mathscr{R}^{\alpha\beta}_{\pm\mp} = \mathscr{R}(\pm P^{\alpha}_{\mathrm{f}}, \mp P^{\beta}_{\mathrm{i}})$ at each of the orthogonal directions of the vector $\boldsymbol{P}_{\mathrm{f}}$, i.e. at $P_{\mathrm{f}} = P^x_{\mathrm{f}}$, P^y_{f}, or P^z_{f}, and at $P_{\mathrm{i}} = P^x_{\mathrm{i}}$, P^y_{i}, or P^z_{i}. The results of 36 possible measurements can be collected into the supermatrix $\mathscr{R}^{\alpha\beta}_{\mu\nu}$, with $\{\alpha,\beta\} = \{x,y,z\}$ and μ,ν denote $+$, or $-$. However, in our simple model there are only 3 independent functions, $|R_{\pm}|$ and $(\chi^r_{+} - \chi^r_{-})$, which can experimentally be determined from this supermatrix, and most of its elements are interrelated.

Indeed, the quantities $|R_{\pm}|$ and $(\chi^r_{+} - \chi^r_{-})$ can be found from measurements of the diagonal elements

$$\mathscr{R}^{yy}_{++} = |R_{+}|^2, \quad \mathscr{R}^{yy}_{--} = |R_{-}|^2, \tag{5}$$

$$\mathscr{R}^{yy}_{+-} = \mathscr{R}^{yy}_{-+} = 0, \tag{6}$$

$$\mathscr{R}^{xx(zz)}_{++} = \mathscr{R}^{xx(zz)}_{--} = |R_{+} + R_{-}|^2/4, \tag{7}$$

$$\mathscr{R}^{xx(zz)}_{+-} = \mathscr{R}^{xx(zz)}_{-+} = |R_{+} - R_{-}|^2/4, \tag{8}$$

$$|R_{+} \pm R_{-}|^2 = |R_{+}|^2 + |R_{-}|^2 \pm 2|R_{+}R_{-}|\cos(\chi^r_{+} - \chi^r_{-}), \tag{9}$$

where it is assumed that $|P_{\mathrm{f}}| = |P^y_{\mathrm{f}}| = 1$ and $|P_{\mathrm{i}}| = |P^y_{\mathrm{i}}| = 1$.

Non-diagonal elements of $\mathscr{R}^{\alpha\beta}_{\mu\nu}$ with $\{\alpha,\beta\} = \{x,z\}$, are as follows:

$$\mathscr{R}^{\alpha\beta}_{++} = \mathscr{R}^{\alpha\beta}_{--} = \mathscr{R}^{\beta\alpha}_{+-} = \mathscr{R}^{\alpha\beta}_{-+}, \tag{10}$$

$$\mathscr{R}^{zx}_{++} = \mathscr{R}^{zx}_{--} = |R_{+} - \mathrm{i}R_{-}|^2/4, \tag{11}$$

$$\mathscr{R}^{zx}_{+-} = \mathscr{R}^{zx}_{-+} = |R_{+} + \mathrm{i}R_{-}|^2/4, \tag{12}$$

$$\mathscr{R}^{y\alpha}_{++} = \mathscr{R}^{y\alpha}_{+-} = \mathscr{R}^{\alpha y}_{++} = \mathscr{R}^{\alpha y}_{-+} = |R_{+}|^2/2, \tag{13}$$

$$\mathscr{R}^{y\alpha}_{--} = \mathscr{R}^{y\alpha}_{-+} = \mathscr{R}^{\alpha y}_{--} = \mathscr{R}^{\alpha y}_{+-} = |R_{-}|^2/2. \tag{14}$$

They do not contain an additional information, but can be used to check the consistency of the model, anticipating that domains are smaller than the lateral projection of the coherence length. If this is not the case, one cannot use Eqs. (5)–(11), and the reflectivity must be calculated for each domain, and afterwards the results should be averaged over the domain distribution [15–17].

If the domains are small, then Eqs. (5)–(14) are valid, but true specular reflection can hardly be discriminated from diffuse scattering within the range of their overlap. As we shall see, the polarization analysis can substantially help to solve this problem. If we assume, that the magnetization of each layer l is decomposed into domains with magnetic moments $\boldsymbol{M}^{\mathrm{l}}$ tilted at a certain angle ϕ with respect to the mean magnetization directed along the applied field $\boldsymbol{H}$ (see Fig. 1), then the strength of this mean field is $B = H + 4\pi M\cos\phi$, with $M = |\boldsymbol{M}^{\mathrm{l}}|$. The components $M^{\mathrm{l}}_x = M\sin\phi$ perpendicular to $\boldsymbol{B}$ are alternating in neighboring domains within each layer, and if the atomic magnetic moments in neighboring layers are coupled antiferromagnetically, as it happens in GMR systems, then M^{l}_x components also change sign from layer to layer. Off-specular scattering from such a system of

domains is concentrated within the range of $Q_{||}r_0 \leqslant 1$ (where r_0 is mean lateral extension of the domains), and has enhancement factor for $q_z d \approx \pi(2n+1)$, where q_z is the wave vector transfer component normal to the surface, d is the multilayer period, and n is integer number.

In the Born approximation (BA) the magnetic scattering operator in Eqs. (2) and (4) reads: $\hat{F}^{\mathrm{l}}_{\mathrm{fi}} = (\boldsymbol{F}^{\mathrm{l}}_{\mathrm{fi}}\boldsymbol{\sigma})$, where $\boldsymbol{F}^{\mathrm{l}}_{\mathrm{fi}} = b_{\mathrm{M}}\mathscr{F}_{\mathrm{M}}(\boldsymbol{Q})\boldsymbol{m}_{\perp}$, b_{M} is the magnetic scattering length density, $\mathscr{F}_{\mathrm{M}}(\boldsymbol{Q}) = \mathscr{F}_{||}(\boldsymbol{Q}_{||})G^{\mathrm{l}}(q_z)$ is the domain form factor with its lateral, $\mathscr{F}_{||}$, and transverse, $G^{\mathrm{l}}(q_z)$, components, $\boldsymbol{m}^{\mathrm{l}}_{\perp} = \boldsymbol{m}^{\mathrm{l}} - \boldsymbol{e}(\boldsymbol{e}\boldsymbol{m}^{\mathrm{l}})$ is the component of the vector $\boldsymbol{m}^{\mathrm{l}} = \boldsymbol{M}^{\mathrm{l}}/M$ perpendicular to the momentum transfer, and $\boldsymbol{e} = \boldsymbol{Q}/|\boldsymbol{Q}|$. At low angles of incidence and scattering, this vector is almost orthogonal to the surface, and thus, to the vector $\boldsymbol{m}^{\mathrm{l}}$. Then, in our model $\boldsymbol{m}^{\mathrm{l}}_{\perp} \approx \boldsymbol{m}^{\mathrm{l}}$ is directed along (or opposite to) the x-axis.

However, BA is invalid at such low angles, that the reflection from the mean potential is sufficiently strong. Then, one should take into account refraction effects and the scattering of the waves reflected from the interfaces. This was done in [15] in the framework of the Distorted Wave BA (DWBA), and the result for each layer l looks as follows:

$$\hat{F}_{\mathrm{fi}} = \hat{t}_{\mathrm{f}}\hat{F}^{tt}\hat{t}_{\mathrm{i}} + \hat{t}_{\mathrm{f}}\hat{F}^{tr}\hat{r}_{\mathrm{i}} + \hat{r}_{\mathrm{f}}\hat{F}^{rt}\hat{t}_{\mathrm{i}} + \hat{r}_{\mathrm{f}}\hat{F}^{rr}\hat{r}_{\mathrm{i}}. \tag{15}$$

Beyond BA, $\hat{F}^{\mathrm{l}}_{\mathrm{fi}}$ is no more a function of only the momentum transfer, but depends on each variable, the incident and scattered wave vectors, separately. The vector $\boldsymbol{F}^{\mathrm{l}}$ in Eq. (4) is not proportional to $\boldsymbol{m}^{\mathrm{l}}_{\perp}$, but receives the components perpendicular to this vector also. For our model, $\boldsymbol{F}^{\mathrm{l}} = \boldsymbol{F}^{\mathrm{l}}_{\mathrm{fi}}$ has, however, only two components:

$$F^{\tau\rho}_{x} = \frac{b_{\mathrm{M}}}{2}(G^{\tau\rho}_{+-} + G^{\tau\rho}_{-+})\mathscr{F}_{||}(\boldsymbol{Q}_{||}), \tag{16}$$

$$F^{\tau\rho}_{z} = \frac{\mathrm{i}b_{\mathrm{M}}}{2}(G^{\tau\rho}_{+-} - G^{\tau\rho}_{-+})\mathscr{F}_{||}(\boldsymbol{Q}_{||}). \tag{17}$$

Here $F^{\tau\rho}_{x(z)}$ are the linear combinations of the transverse form-factors $G^{\tau\rho}_{\mu\nu}$ with $\{\tau,\rho\} = \{t,r\}$:

$$G^{tt}_{\mu\nu} = \{\mathrm{e}^{\mathrm{i}(p^{\mathrm{f}}_{\mathrm{l}\mu} + p^{\mathrm{i}}_{\mathrm{l}\nu})a_{\mathrm{l}}} - 1\}/\mathrm{i}(p^{\mathrm{f}}_{\mathrm{l}\mu} + p^{\mathrm{i}}_{\mathrm{l}\nu}), \tag{18}$$

$$G^{tr}_{\mu\nu} = \{\mathrm{e}^{\mathrm{i}(p^{\mathrm{f}}_{\mathrm{l}\mu} - p^{\mathrm{i}}_{\mathrm{l}\nu})a_{\mathrm{l}}} - 1\}/\mathrm{i}(p^{\mathrm{f}}_{\mathrm{l}\mu} - p^{\mathrm{i}}_{\mathrm{l}\nu}), \tag{19}$$

$$G^{rt}_{\mu\nu} = -\{\mathrm{e}^{-\mathrm{i}(p^{\mathrm{f}}_{\mathrm{l}\mu} - p^{\mathrm{i}}_{\mathrm{l}\nu})a_{\mathrm{l}}} - 1\}/\mathrm{i}(p^{\mathrm{f}}_{\mathrm{l}\mu} - p^{\mathrm{i}}_{\mathrm{l}\nu}), \tag{20}$$

$$G^{rr}_{\mu\nu} = -\{\mathrm{e}^{-\mathrm{i}(p^{\mathrm{f}}_{\mathrm{l}\mu} + p^{\mathrm{i}}_{\mathrm{l}\nu})a_{\mathrm{l}}} - 1\}/\mathrm{i}(p^{\mathrm{f}}_{\mathrm{l}\mu} + p^{\mathrm{i}}_{\mathrm{l}\nu}), \tag{21}$$

where a_{l} is the layer thickness.

It is important to note that scattering in our model is always associated with transition between different spin states denoted by $\{\mu,\nu\} = \{+,-\}$. Therefore the functions $G^{tt}_{\mu\nu}$ and $G^{rr}_{\mu\nu}$ depend on corresponding "ordinary" wave vector transfers $q^{z}_{\mu\nu} = p^{\mathrm{f}}_{\mu} + p^{\mathrm{i}}_{\nu}$, while the functions $G^{tr}_{\mu\nu}$ and $G^{rt}_{\mu\nu}$ depend on the "anomalous" ones: $\tilde{q}^{z}_{\mu\nu} = p^{\mathrm{f}}_{\mu} - p^{\mathrm{i}}_{\nu}$.

Substitution Eqs. (15)–(21) into Eqs. (4) and (2) yields a general equation for the scattering cross sections [15], whose diagonal elements are written in the form similar to Eqs. (5)–(9):

$$\frac{\mathrm{d}\sigma^{yy}}{\mathrm{d}\Omega_{++}} = \frac{\mathrm{d}\sigma^{yy}}{\mathrm{d}\Omega_{--}} = 0, \tag{22}$$

$$\frac{\mathrm{d}\sigma^{yy}}{\mathrm{d}\Omega_{+-}} = |F_x - \mathrm{i}F_z|^2, \tag{23}$$

$$\frac{\mathrm{d}\sigma^{yy}}{\mathrm{d}\Omega_{-+}} = |F_x + \mathrm{i}F_z|^2, \tag{24}$$

$$\frac{\mathrm{d}\sigma^{xx(zz)}}{\mathrm{d}\Omega_{++}} = \frac{\mathrm{d}\sigma^{xx(zz)}}{\mathrm{d}\Omega_{--}} = |F_{x(z)}|^2, \tag{25}$$

$$\frac{\mathrm{d}\sigma^{xx(zz)}}{\mathrm{d}\Omega_{+-}} = \frac{\mathrm{d}\sigma^{xx(zz)}}{\mathrm{d}\Omega_{-+}} = |F_{z(x)}|^2. \tag{26}$$

From these equations it follows that, if at polarization along the field (see, Fig. 2a) off-specular scattering is not detected in non-spin-flip channel, but is found in spin-flip channels (see Figs. 2b,c), then one still needs to accomplish a set of additional measurements in order to obtain all possible information on the source of scattering. This set must include the experiment, with the polarization perpendicular to the mean magnetization. Indeed, the amplitudes $F_{x(z)} = |F_{x(z)}|\exp(\mathrm{i}\chi_{x(z)})$ are complex functions and the model is characterized by two absolute values $|F_{x(z)}|$ and by two phases $\chi_{x(z)}$. According to general principles, both of the phases cannot be determined, but the phase shift $(\chi_x - \chi_z)$ can be found. However, this is impossible to do using only Eqs. (22)–(24), and one needs to employ one of Eqs. (25) and (26).

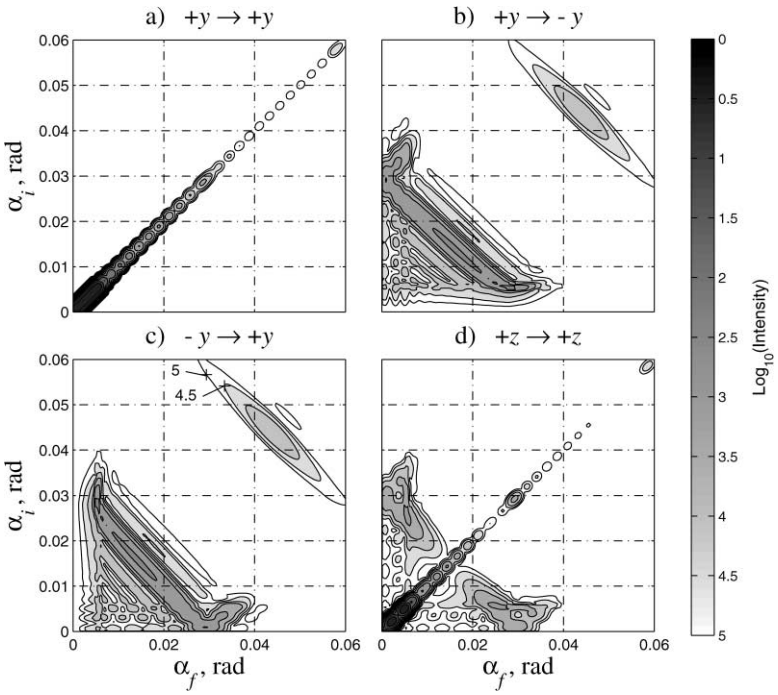

Fig. 2. Intensity distribution of (a–c) specular reflection (non-spin-flip) and off-specular scattering (spin-flip) for polarization along the field; (d) non-spin-flip reflection and scattering polarization perpendicular to the field, calculated for the model in Fig. 1.

All the other (nondiagonal) components of the scattering cross section supermatrix $(\mathrm{d}\sigma/\mathrm{d}\Omega)^{\alpha\beta}_{\mu\nu}$ do not contain new information on the domain model under consideration. If either $\boldsymbol{P}_\mathrm{i}$, or/and $\boldsymbol{P}_\mathrm{f}$ is directed perpendicular to the field, i.e. $\{\alpha,\beta\} = \{x,z\}$, then

$$\frac{\mathrm{d}\sigma^{\alpha\beta}}{\mathrm{d}\Omega_{++}} = \frac{\mathrm{d}\sigma^{\alpha\beta}}{\mathrm{d}\Omega_{--}} = |F_x + F_z|^2/2, \tag{27}$$

$$\frac{\mathrm{d}\sigma^{\alpha\beta}}{\mathrm{d}\Omega_{+-}} = \frac{\mathrm{d}\sigma^{\alpha\beta}}{\mathrm{d}\Omega_{-+}} = |F_x - F_z|^2/2. \tag{28}$$

$$\frac{\mathrm{d}\sigma^{\alpha y}}{\mathrm{d}\Omega_{++}} = \frac{\mathrm{d}\sigma^{\alpha y}}{\mathrm{d}\Omega_{-+}} = \frac{\mathrm{d}\sigma^{y\alpha}}{\mathrm{d}\Omega_{--}} = \frac{\mathrm{d}\sigma^{y\alpha}}{\mathrm{d}\Omega_{-+}} = |F_x + \mathrm{i}F_z|^2/2, \tag{29}$$

$$\frac{\mathrm{d}\sigma^{\alpha y}}{\mathrm{d}\Omega_{-}} = \frac{\mathrm{d}\sigma^{\alpha y}}{\mathrm{d}\Omega_{+-}} = \frac{\mathrm{d}\sigma^{y\alpha}}{\mathrm{d}\Omega_{++}} = \frac{\mathrm{d}\sigma^{y\alpha}}{\mathrm{d}\Omega_{+-}} = |F_x - \mathrm{i}F_z|^2/2. \tag{30}$$

Some examples of the numerical results simulating the experimental observations in Ref. [6] are depicted in Figs. 2a–c, where the intensity distribution is plotted as a function of the incident angle α_i and the angle of scattering α_f ($p_0^{\mathrm{f,i}} = 2\pi/\lambda$ and λ is the neutron wave length). In those experiments, no off-specular scattering was detected at the incoming and outgoing polarizations directed along with (similar Fig. 2a), or opposite (not shown) to the field. On the contrary, spin-flip reflectivities $\mathscr{R}^{yy}_{+-(-+)} = 0$, while off-specular scattering is rather strong, and the intensity distribution in Figs. 2b,c reveal a number of remarkable features. Thus, one can clearly see two antiferromagnetic Bragg sheets along which $(p^{\mathrm{i}}_{\pm} + p^{\mathrm{f}}_{\mp})d \approx \pi,3\pi$, and a set of low intensity sheets running parallel to the Bragg ones. The distance between them is determined by the total thickness of the system.

The other prominent property of Figs. 2b,c is that the intensity distribution is quite asymmetric. This is due to the asymmetry in the spin-flip scattering amplitude F_z with respect to interchange of the incident and outgoing wave numbers. It is important to remind that in BA, the amplitudes are

real functions of the wave vector transfer. This, however, does not hold for DWBA, which takes into account the fact that the refraction effect for the incoming wave (positive spin projection) is higher than that for the scattered one, if its spin projection onto the field direction is negative. The effect is mostly pronounced close to the total reflection, while at higher wave vector transfer the symmetry is almost completely restored. The results is Fig. 2c are complementary to those in Fig. 2b and show, that interchange P_{f}^{y} with P_{i}^{y} is equivalent with interchange p_{f} with p_{i}, as follows from the reciprocity principle.

The other effect of DWBA seen in Figs. 2b,c is manifested by a short "anomalous" Bragg sheet running perpendicular to the "ordinary" ones, and positioned at $(p_{\mathrm{i}}^{+} - p_{\mathrm{f}}^{-})d \approx \pi$. It arises due to the scattering of the waves reflected from the interfaces. It has appreciable intensity only in the range of strong reflection and is seen in Fig. 2b only at low angles of exit. The other process, i.e. reflection of the waves scattered from domains, is rather weak. At low angles of exit, one can also see some modulation of the intensity which is due to the interference of the fringes running parallel to the "ordinary" and "anomalous" Bragg sheets.

The intensity distribution in Fig. 2d is, in contrast to that in Figs. 2b,c is rather symmetrical and contains both specular and off-specular components. However, diffuse scattering at the position of specular reflection is heavily suppressed and does not interfere with the reflection process. Indeed, from Eq. (26) and (17) it follows that in this case non-spin-flip diffuse scattering cross section is due to the virtual transitions between two spin states. However at $p_0^{\mathrm{i}} = p_0^{\mathrm{f}}$ these processes are absolutely equivalent, exactly compensate each other, and $F_z^{\mathrm{l}} = 0$. The off-specular scattering is concentrated close to the range of the total reflection with respect to the incidence, or scattering, while it becomes invisible in the range of BA validity.

3. Conclusions

In summary, we have shown, that 3D polarization analysis is useful to obtain the unique solution of the model of magnetic arrangements in multilayers. In particular, even one experiment with the polarization perpendicular to the mean magnetization carried out in addition to the measurements with polarization along the magnetization allows to determine all possible components of the reflectance and the scattering amplitudes for the model of antiferromagnetic domains.

Acknowledgements

This work was supported by the German BMBF, Russian State Program for Statistical Physics (Grant VIII-2), RFBR Grants No. 00-02-16873 and 00-15-96814, and the Russian Program "Neutron Studies of Condensed Matter".

References

[1] G.P. Felcher, R.O. Hilleke, R.K. Crawford, J. Haumann, R. Kleb, G. Ostrowski, Rev. Sci. Instrum. 58 (1987) 609.
[2] C.F. Majkrzak, Physica B 221 (1996) 342.
[3] A. Schreyer, J.F. Ankner, Th. Zeidler, H. Zabel, C.F. Majkrzak, M. Schäfer, P. Grünberg, Europhys. Lett. 32 (1995) 595.
[4] A. Schreyer, J.F. Ankner, Th. Zeidler, H. Zabel, M. Schäfer, J.A. Wolf, P. Grünberg, C.F. Majkrzak, Phys. Rev. B 52 (1995) 16066.
[5] W. Hahn, M. Loewenhaupt, G.P Felcher, Y.Y. Huang, S.S. Parkin, J. Appl. Phys. 75 (1994) 3564.
[6] V. Lauter-Pasyuk, H.J. Lauter, B. Toperverg, O. Nikonov, E. Kravtsov, M.A. Milyaev, L. Romashev, V. Ustinov, Physica B 238 (2000) 194.
[7] V. Lauter-Pasyuk, H.J. Lauter, B. Toperverg, O. Nikonov, E. Kravtsov, M.A. Milyaev, L. Romashev, V. Ustinov, Physica B, these Proceedings.
[8] J.A. Borchers J.A. Dura, C.F. Majkrzak, S.Y. Hsu, R. Lolee, W.P. Pratt, J. Bass, Physica B 283 (2000) 162.
[9] A.I. Okorokov, Physica B, these Proceedings.
[10] W.H. Kraan, M.Th. Rekveldt, V.A. Ul'yanov, L.A. Akselrod, G.P. Gordeev, V.M. Pusenkov, Physica B 267–268 (1999) 75.
[11] F. Tasset, Physica B, these Proceedings.
[12] C.S. Schneider, C.G. Shull, Phys. Rev. B 3 (1971) 830.
[13] G.P. Felcher et al., Nature 377 (1995) 409.
[14] L. Akselrod, G. Gordeev, V. Zabenkin, I. Lazebnik, B. Toperverg, Physica B 174 (1991) 349.
[15] B.P. Toperverg, A. Rühm, W. Donner, H. Dosch, Physica B 267–268 (1999) 198.
[16] A. Rühm, B. Toperverg, H. Dosch, Phys. Rev. B 60 (1999) 16073.
[17] B.P. Toperverg, Physica B, these Proceedings.